

Electronic structure of graphene and doping effect on SiO₂

Yong-Ju Kang, Joongoo Kang, and K. J. Chang

Department of Physics, Korea Advanced Institute of Science and Technology, Daejeon 305-701, Korea

(Received 11 April 2008; revised manuscript received 7 August 2008; published 4 September 2008)

First-principles calculations show that the electronic structure of graphene on SiO₂ strongly depends on the surface polarity and interface geometry. Surface dangling bonds mediate the coupling to graphene and can induce hole or electron doping via charge transfer even in the absence of extrinsic impurities in substrate. In an interface geometry where graphene is weakly bonded to an O-polar surface, graphene is *p* doped, whereas *n* doping takes place on a Si-polar surface with active dangling bonds. We suggest that electron and hole doping domains observed on SiO₂ are related to different surface polarities.

DOI: [10.1103/PhysRevB.78.115404](https://doi.org/10.1103/PhysRevB.78.115404)

PACS number(s): 73.40.Gk, 73.40.Ty, 77.22.Jp, 77.84.Bw

I. INTRODUCTION

Graphene, a monolayer of carbon atoms packed in a honeycomb lattice, has a unique electronic structure with a zero gap and quasiparticles behaving like massless Dirac fermions.^{1,2} The low-energy band structure of graphene near two inequivalent Brillouin-zone corners is characterized as cones with the linear dispersion. It has been demonstrated that graphene is a promising material for future nanoscale devices.^{3,4} For applications to electrical and optical devices, it is important to control the band gap, carrier type, and concentration.

Graphene can be doped by using electrical gates, substrates, and chemical species such as atoms and molecules.²⁻⁷ Experiments have reported that graphene grown on a SiC surface interacts with the substrate, being *n* doped and exhibiting a gap of about 0.26 eV.⁸ It has been shown theoretically that the first carbon layer on SiC acts as a buffer layer, and that the graphene nature of the film is recovered by the second carbon layer.^{9,10} For graphene supported on SiO₂, scanning probe microscopy images showed that structural corrugations partially conform to the underlying morphology of the substrate.¹¹ The observation of electron and hole doping domains suggests that the carrier density in graphene varies with the spatial distribution of disorders or charged impurities.¹²⁻¹⁴ Despite the expectation that graphene is coupled to SiO₂, it is not fully understood how SiO₂ surfaces interact with graphene and modify the electronic properties of graphene layers.

In this work, first-principles theoretical calculations are performed to investigate the electronic structure of single and bilayer graphene on Si- and O-terminated SiO₂ (0001) surfaces. For a single layer of graphene, we show that *p* and *n* doping effects can be solely induced via charge transfer on O- and Si-polar surfaces with active dangling bonds, respectively, without extrinsic impurities that are widely thought as doping sources. In bilayer systems, the characteristics of the first carbon layer vary with the surface polarity and interface geometry, while the second layer is mostly affected by the type of induced doping. Our calculations provide a clue for understanding the electron-hole puddles and different doping domains observed in graphene on SiO₂.

II. CALCULATION METHOD

The first-principles calculations were performed using the local-density-functional approximation (LDA)^{15,16} for the

exchange-correlation potential and ultrasoft pseudopotentials,¹⁷ as implemented in the VASP code.¹⁸ The wave functions were expanded in plane waves up to a cutoff of 396 eV. Using slab geometry, graphene layers were placed on a α -quartz SiO₂ (0001) surface with Si- or O-polarity, and the back side of the slab was passivated by hydrogen. The supercell consisted of single or double graphene layers, 14 bilayers of SiO₂, and a vacuum region of 20 Å. Due to the small lattice mismatch between the graphene and α -quartz SiO₂, which have the lattice constants of 2.46 and 4.91 Å, respectively, a lateral 2 × 2 cell can lead to the periodically repeated geometry. The Brillouin-zone integration was performed using a set of *k* points generated by the 6 × 6 × 1 Monkhorst-Pack mesh, and the ionic coordinates were fully relaxed until the residual forces were less than 0.03 eV/Å.

III. RESULTS AND DISCUSSION

On the Si-terminated surface, a single graphene layer has the lowest energy when the hexagon centers are positioned directly above the surface Si atoms [Fig. 1(a)] at a distance of 3.29 Å from the substrate. As this disconnection is much larger than the bond length of 1.87 Å in SiC, interactions between the graphene and substrate atoms are extremely weak and do not form Si-C bonds. The binding energy with respect to free-standing graphene was calculated to be 20 meV per C atom. In a different interface geometry, where the graphene C atoms are located on top of the surface Si atoms, the energy is only higher by approximately 3 meV per C

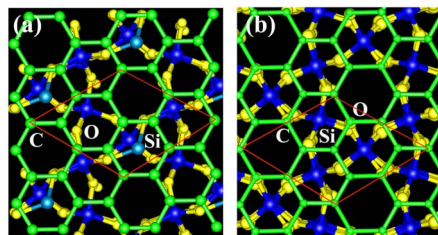


FIG. 1. (Color online) Top view of a single graphene layer on (a) Si-terminated and (b) O-terminated SiO₂ surfaces. The blue (dark), yellow (white), and green (gray) balls denote the Si, O, and C atoms, respectively. The red lines represent the 2 × 2 graphene unit cell.

atom. In the 2×2 unit cell, there is only one surface Si atom bonded to two substrate O atoms with bond lengths of 1.63 and 1.67 Å, as compared to the bulk value of 1.61 Å in SiO₂. Due to two dangling bonds per surface Si atom, the Si-terminated surface is chemically inactive and thus does not affect the structural and electronic properties of graphene.

On the other hand, on the O-terminated surface, the 2×2 cell contains two surface O atoms with Si-O bond lengths of 1.61 Å. As each O atom has one dangling bond, the O-terminated surface is chemically reactive and strongly interacts with the graphene layer. In the lowest-energy configuration [Fig. 1(b)], the C atoms placed on top of the surface O atoms relax toward the substrate and form strong C-O bonds with a bond length of 1.45 Å. These C-O bonds severely distort the planar structure of the graphene layer. The binding energy substantially increases to 0.78 eV per C atom, a value that is much larger compared to those previously calculated for a graphene layer on a SiC substrate.¹⁰ When the carbon layer laterally shifts by $(\mathbf{a}_1 + \mathbf{a}_2)/3$ on the surface, where \mathbf{a}_1 and \mathbf{a}_2 are the graphene primitive lattice vectors, a metastable interface can form, where one O atom is located below a graphene C atom and forms a weak C-O bond. The other O, however, which is initially positioned below the hexagon center, relaxes toward a neighboring C atom. Due to the weak coupling to the substrate, graphene nearly maintains the planar geometry at a distance of 2.58 Å from the substrate. The bonding gives an energy gain of 0.13 eV per C atom, which is six times larger than that on the Si-terminated surface. In a stable configuration, a graphene layer with strong C-O bonds will be more rigid against lateral displacement compared to a metastable interface geometry.

The electronic band structures of a single graphene layer on the Si- and O-terminated surfaces are compared in Figs. 2(a) and 2(c). As expected, the linear bands near the Dirac point are maintained on the Si-terminated surface due to the very weak coupling of graphene to the substrate. As no charge transfer occurs between the graphene and substrate, the Fermi level lies at the Dirac point. The localized bands around -2 and 2 eV are related to the bonding and antibonding states of the two surface dangling bonds, respectively, compared to the projected bands (shaded areas) of SiO₂. On the other hand, on the O-terminated surface, strong interactions between the C and surface O atoms significantly modify the linear band structure of graphene. In this stable geometry, the degeneracy at the Dirac point is removed with the energy splitting of 2.85 eV. The electronic characteristics of graphene disappear completely, as shown in Fig. 2(c). In the metastable geometry, the linear bands of graphene are generally maintained [Fig. 3(a)]. However, as the surface O atoms interact more strongly with one sublattice site of graphene than with the other sublattice, the graphene sublattice symmetry is broken, resulting in a small gap of 0.13 eV at the Dirac point. When the 4×4 cell is used, where the density of the weak C-O bonds is reduced by a factor of 4 by saturating the O dangling bonds by hydrogen, the energy gap is found to be 0.04 eV. This result is consistent with the recent theoretical prediction that the energy splitting at the Dirac point is proportional to the density of disorders.¹⁹ It is interesting to note that charge transfer occurs from graphene

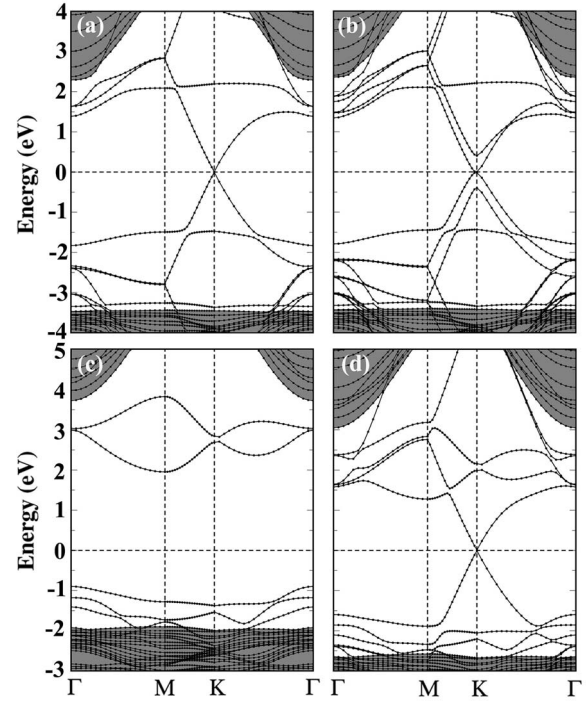


FIG. 2. Band structures of (a) single and (b) bilayer graphene on the Si-terminated SiO₂ surface are compared with those of the stable interface geometries of (c) single and (d) bilayer graphene on the O-terminated surface. The shaded regions represent the projected bands of bulk SiO₂, and the Fermi levels are set to zero.

to substrate, thus, the Fermi level is lowered, with its position varying with the amount of transferred charges. As a consequence of the charge transfer, the O-terminated surface induces *p*-type doping in the carbon sheet.

For a single layer of graphene on SiO₂, recent scanning tunneling microscopy (STM) studies showed the presence of a strong spatially dependent perturbation, which breaks the hexagonal lattice symmetry.¹¹ Both hexagonal and triangular lattice patterns were observed in close proximity. We examine the distribution of charge densities near the Dirac point,

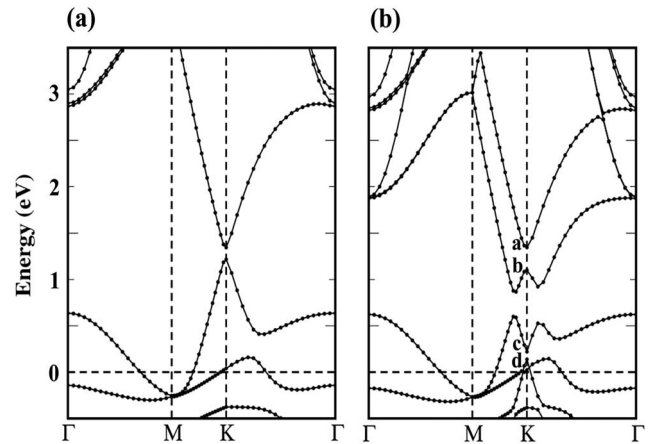


FIG. 3. Energy-band spectrum of (a) single and (b) bilayer graphene in the metastable interface geometry on the O-terminated surface, with the Fermi levels set to zero.

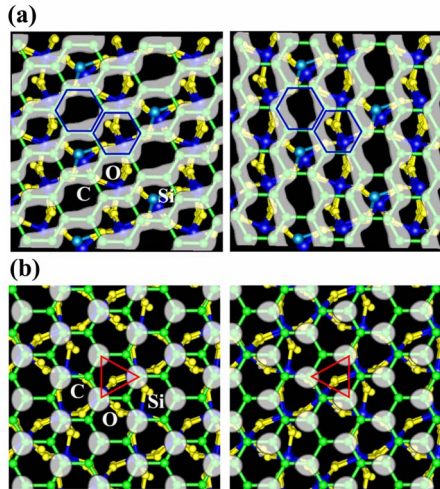


FIG. 4. (Color online) Isosurfaces (white clouds) of the charge densities of two states just near the Dirac point for a single layer of graphene (a) on the inactive Si-terminated surface and (b) in the metastable interface geometry on the O-terminated surface. The blue and red lines (black) represent the hexagonal and triangular patterns of the charge distribution, respectively. The green balls in the clouds denote the C atoms, whereas blue (dark) and yellow (white) balls denote the Si and O atoms, respectively.

and find that the hexagonal patterns appear for a single layer of graphene on the inactive Si-polar surface [Fig. 4(a)]. As the triangular patterns appear in the metastable interface geometry on the O-polar surface [Fig. 4(b)], these images are attributed to the weak interaction of graphene with the substrate, which breaks the sublattice symmetry and thus induces the gap opening.

When a second carbon layer is placed in the *AB* stacking of graphite on the Si-terminated surface, the distance between the two graphene layers is 3.27 Å, as compared to the bulk graphite value of 3.35 Å. Due to weak interlayer interactions, the bilayer graphene exhibits parabolic bands around the Fermi level [Fig. 2(b)], which resemble those of pristine bilayer graphene.²⁰ On the O face, the electronic structure of the second carbon layer in the *AB* stacking strongly depends on the interface geometry between the first layer and the substrate. In the stable interface configuration [Fig. 1(b)], the second carbon layer is positioned at a distance of 3.47 Å and exhibits the linear band characteristics of free-standing graphene, as shown in Fig. 2(d). As the active O-terminated surface is almost completely passivated, the first carbon layer acts as a buffer layer, similar to the case of double graphene layers on a C-terminated SiC surface.^{9,10} In fact, the Fermi level lies at the Dirac point, indicating that the substrate effect on the energy spectrum of the second carbon sheet is perfectly shielded.

In the metastable interface structure on the O face, the second carbon layer interacts weakly with the first carbon layer at an interlayer distance of 3.32 Å. However, owing to the substrate-induced hole doping in the first carbon layer, the symmetry between the two layers is broken by the dipole field, which is generated across the interface by accumulated electron charges on the substrate and depleted charges on the first carbon layer. Due to the difference (U) in the on-site

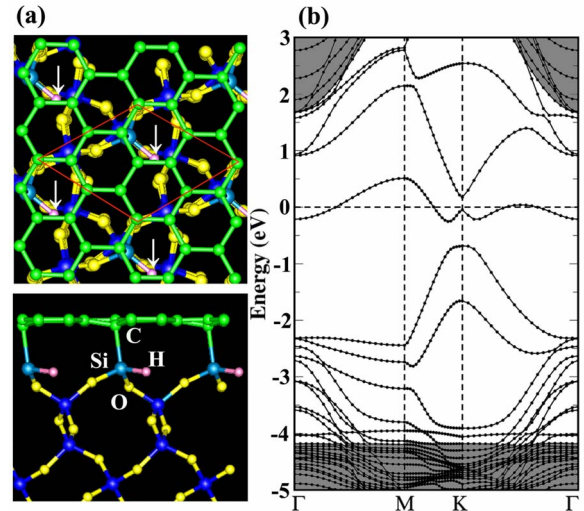


FIG. 5. (Color online) (a) Atomic structure of single graphene and (b) energy-band spectrum of bilayer graphene on the partially hydrogenated Si-polar surface, with the Fermi level set to zero. The blue (dark), yellow (white), and green (gray) balls denote the Si, O, and C atoms, respectively, whereas the H atoms are indicated by arrows. The red lines represent the 2×2 graphene unit cell.

Coulomb potentials of the two layers,^{7,21,22} the energy band associated with the second carbon layer is lowered by $U = 0.79$ eV with respect to that of the first carbon layer [Fig. 3(b)]. Thus, the Fermi level lies at 0.73 eV below the middle of the energy gap. For the four graphene states labeled *a*, *b*, *c*, and *d* at the *K* point in the Brillouin zone, the electron charges of the two higher levels (*a* and *b*) are mainly distributed on the carbon sheet next to the interface while the lower levels (*c* and *d*) are related to the second carbon sheet. Except for the position of the Fermi level, the electronic structure of the bilayer graphene on the O face is very similar to that for a *K*-doped bilayer of graphene on a SiC substrate.⁷ The energy gap of 0.28 eV results from the interlayer bonding which is induced by the symmetry-breaking field compared to the single layer case in which the energy gap opens only through the breaking of the sublattice symmetry.

For a single graphene layer, surface dangling bonds play an important role in the coupling of graphene to substrate. Although the Si face is chemically inactive, it can become an active surface if one of the two dangling bonds at each surface Si atom is passivated by hydrogen. In the optimized geometry [Fig. 5(a)], the graphene C atoms are slightly displaced toward the substrate to form strong Si-C bonds with a bond length of 2.01 Å. The binding energy is enhanced by 0.18 eV per C atom, as compared to the Si face without hydrogenation. Interestingly, it was found that the graphene on the partially hydrogenated Si face is *n* doped, with the Fermi level positioned in the graphene conduction band [Fig. 5(b)], in contrast to that on the O face. Here, partially hydrogenated Si face is similar to the Si-terminated SiC surface, which has one dangling bond per surface Si atom and induces electron doping.^{9,10} An analysis of the charge densities shows that electron charges are mostly depleted from the surface Si layer. As the hydrogenated surface Si atoms are only covalently bonded to one sublattice atom of graphene,

the breaking of the sublattice symmetry is significant, resulting in an energy splitting of 1.2 eV at the Dirac point. As discussed earlier, this large gap results from the high density of the Si-C bonds,¹⁹ i.e., one Si-C bond per 2×2 cell, and from the strong interactions between the graphene C and surface Si atoms. Using the 4×4 cell containing one Si-C bond, we note that the energy gap decreases to 0.5 eV. If the density of active dangling bonds lies in the dilute limit by reducing the hydrogenation level, the energy gap will be reduced considerably.²³ In this case, the electron-doping effect is expected to remain due to the charge transfer from the Si dangling bonds to the graphene. For a second carbon layer placed in the *AB* stacking, an energy gap of 0.50 eV was observed, which results from the electron doping effect.

Recently, electron-hole puddles or doping domains were observed in graphene on SiO₂ surfaces and were attributed to charged impurities or disorders.¹²⁻¹⁴ Our calculations indicate that hole and electron doping domains can be formed by the active dangling bonds of the surface O and Si atoms, respectively, even in the absence of charged impurities in the substrate. Thus, the observation of electron-hole puddles¹² may be related to different surface polarities on corrugated SiO₂ substrates. In two-dimensional graphene, intrinsic ripples and corrugation appear spontaneously owing to thermal fluctuation and supported substrate, as observed by experiments.^{24,25} Here we point out that only buckling and oscillation in graphene do not give rise to the doping effect. In theoretical calculations,²⁶ where interactions between graphene and substrate were not included, ripples only modify the low-energy electronic structure of graphene, without altering the charge neutrality point.

Finally, we address that our calculations are in the regime of strong interactions of graphene with idealized crystalline SiO₂ surfaces. In real experiments, graphene layers are usually deposited on the amorphous surface of SiO₂, which loses periodicity and polarity. Because of the computational demand, it is difficult to perform first-principles calculations

for exfoliated graphene on amorphous SiO₂ substrate at this point. However, we point out that the results provide useful information on the realistic graphene-substrate interaction. It was recently shown that the linear dispersion of single layer graphene is preserved in misoriented multilayer systems despite the presence of interlayer interactions.²⁷ If graphene is misoriented on a perfect crystalline SiO₂ surface, one may expect that a similar decoupling effect occurs between the graphene and substrate. In fact, in the metastable interface configuration on the O-polar surface, it was shown that a lateral displacement of graphene greatly weakens the graphene-substrate interaction, while the strong C-O bonds are formed when the C atoms are positioned on top of the O atoms. On amorphous SiO₂ substrate, although the Si or O dangling bonds may be locally active, their activities are expected to be suppressed in the whole system due to irregular orientations. In this case, although the graphene-substrate interaction will be weakened, the local *p*-type doping effect is still expected in the presence of the O dangling bonds.

IV. CONCLUSIONS

In this work, we found that carbon layers behave as free-standing graphene on the Si-terminated surface with inactive dangling bonds. As the O-terminated surface is chemically reactive, the characteristics of the first carbon layer are significantly modified by the formation of the strong C-O bonds, whereas the Dirac fermion nature is recovered with the second carbon layer. In the metastable interface geometry on the O face, the substrate is weakly bonded to the first carbon layer and induces the *p*-type doping, which is attributed by the charge transfer from the graphene to the oxygen dangling bonds. It was suggested that graphene can be *n* doped if the Si-terminated surface has active dangling bonds.

ACKNOWLEDGMENT

This work was supported by the Korea Research Foundation Grant No. KRF-2005-084-C00007.

¹K. S. Novoselov, A. K. Geim, S. V. Morozov, D. Jiang, M. I. Katsnelson, I. V. Grigorieva, S. V. Dubonos, and A. A. Firsov, *Nature (London)* **438**, 197 (2005).

²Y. Zhang, Y.-W. Tan, H. L. Stormer, and P. Kim, *Nature (London)* **438**, 201 (2005).

³C. Berger, Z. Song, T. Li, X. Li, A. Y. Ogbazghi, R. Feng, Z. Dai, A. N. Marchenkov, E. H. Conrad, P. N. First, and W. A. de Heer, *J. Phys. Chem. B* **108**, 19912 (2004).

⁴C. Berger, Z. Song, X. Li, X. Wu, N. Brown, C. Naud, D. Mayou, T. Li, J. Hass, A. N. Marchenkov, E. H. Conrad, P. N. First, and W. A. de Heer, *Science* **312**, 1191 (2006).

⁵X. Li, X. Wang, L. Zhang, S. Lee, and H. Dai, *Science* **319**, 1229 (2008).

⁶K. S. Novoselov, A. K. Geim, S. V. Morozov, D. Jiang, Y. Zhang, S. V. Dubonos, I. V. Grigorieva, and A. A. Firsov, *Science* **306**, 666 (2004).

⁷T. Ohta, A. Bostwick, T. Seyller, K. Horn, and E. Rotenberg, *Science* **313**, 951 (2006).

⁸S. Y. Zhou, G.-H. Gweon, A. V. Fedorov, P. N. First, W. A. De Heer, D.-H. Lee, F. Guinea, A. H. Castro Neto, and A. Lanzara, *Nat. Mater.* **6**, 770 (2007).

⁹F. Varchon, R. Feng, J. Hass, X. Li, B. N. Nguyen, C. Naud, P. Mallet, J.-Y. Veullen, C. Berger, E. H. Conrad, and L. Magaud, *Phys. Rev. Lett.* **99**, 126805 (2007).

¹⁰A. Mattausch and O. Pankratov, *Phys. Rev. Lett.* **99**, 076802 (2007).

¹¹M. Ishigami, J. H. Chen, W. G. Cullen, M. S. Fuhrer, and E. D. Williams, *Nano Lett.* **7**, 1643 (2007).

¹²J. Martin, N. Akerman, G. Ulbricht, T. Lohmann, J. H. Smet, K. Von Klitzing, and A. Jacoby, *Nat. Phys.* **4**, 144 (2008).

¹³C. Casiraghi, S. Pisana, K. S. Novoselov, A. K. Geim, and A. C. Ferrari, *Appl. Phys. Lett.* **91**, 233108 (2007).

¹⁴C. Stampfer, F. Molitor, D. Graf, K. Ensslin, A. Jungen, C. Hierold, and L. Wirtz, *Appl. Phys. Lett.* **91**, 241907 (2007).

¹⁵W. Kohn and L. J. Sham, *Phys. Rev.* **140**, A1133 (1965).

¹⁶D. M. Ceperley and B. J. Alder, *Phys. Rev. Lett.* **45**, 566 (1980).

- ¹⁷D. Vanderbilt, Phys. Rev. B **41**, 7892 (1990).
- ¹⁸G. Kresse and J. Furthmüller, Phys. Rev. B **54**, 11169 (1996).
- ¹⁹J. Kang, J. Bang, B. Ryu, and K. J. Chang, Phys. Rev. B **77**, 115453 (2008).
- ²⁰S. Latil and L. Henrard, Phys. Rev. Lett. **97**, 036803 (2006).
- ²¹E. McCann, Phys. Rev. B **74**, 161403(R) (2006).
- ²²E. V. Castro, K. S. Novoselov, S. V. Morozov, N. M. R. Peres, J. M. B. Lopes dos Santos, J. Nilsson, F. Guinea, A. K. Geim, and A. H. Castro Neto, Phys. Rev. Lett. **99**, 216802 (2007).
- ²³The defect density of one Si-C bond per 20×20 cell can give rise to the measured carrier concentration of $4 \times 10^{12} \text{ cm}^{-2}$ in Ref. 16. Using the linear variation of the energy gap with the defect density in Ref. 21, the energy gap is estimated to be about 20 meV for the 20×20 cell, nearly recovering the Dirac fermion nature of graphene.
- ²⁴J. C. Meyer, A. K. Geim, M. I. Katsnelson, K. S. Novoselov, T. J. Booth, and S. Roth, Nature (London) **446**, 60 (2007).
- ²⁵E. Stolyarova, K. T. Rim, S. Ryu, J. Maultzsch, P. Kim, L. E. Brus, T. F. Heinz, M. S. Hybertsen, and G. W. Flynn, Proc. Natl. Acad. Sci. U.S.A. **104**, 9209 (2007).
- ²⁶T. O. Wehling, A. V. Balatsky, M. I. Katsnelson, and A. I. Lichtenstein, arXiv:0710.5828 (unpublished).
- ²⁷S. Latil, V. Meunier, and L. Henrard, Phys. Rev. B **76**, 201402(R) (2007).